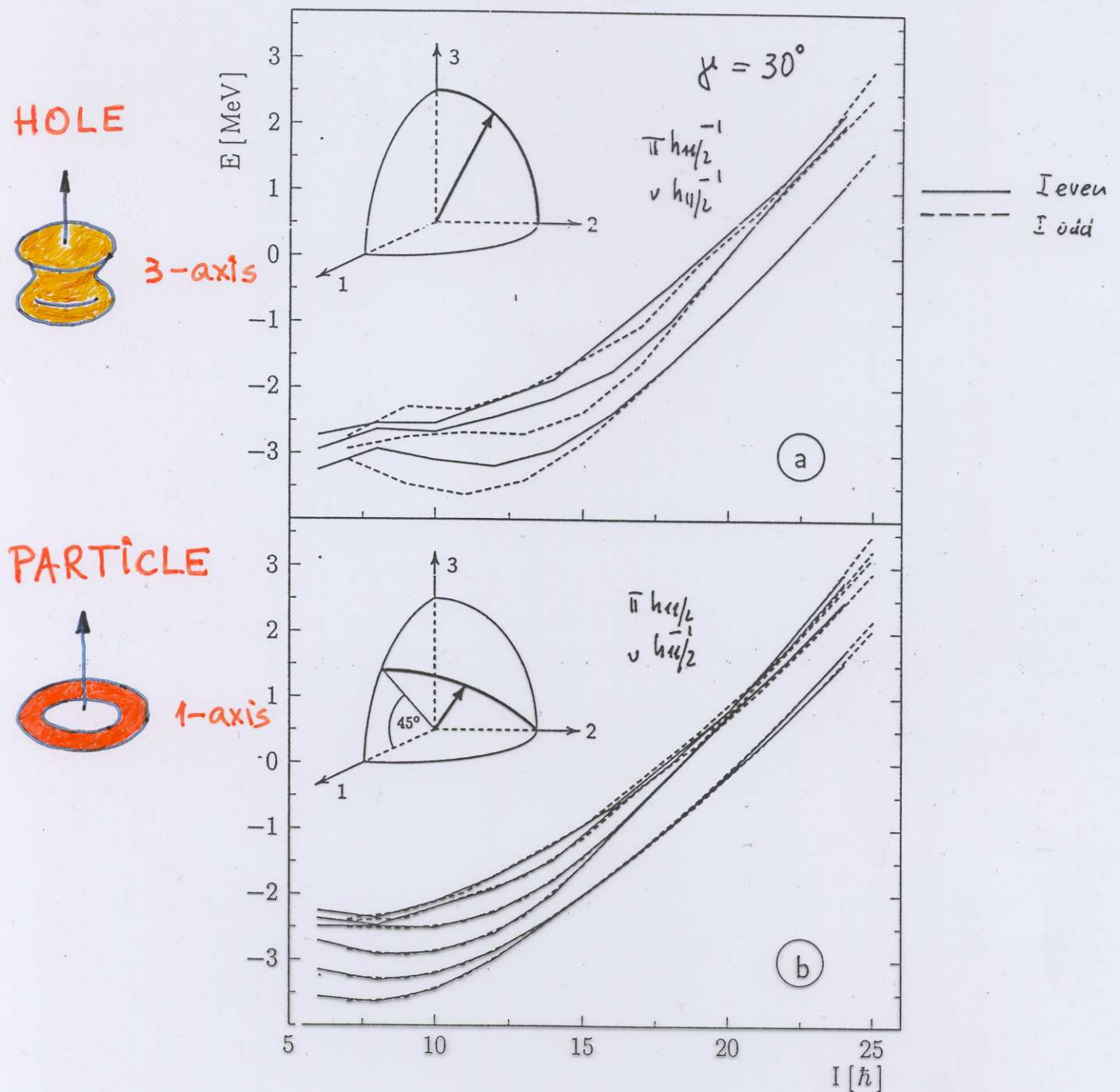
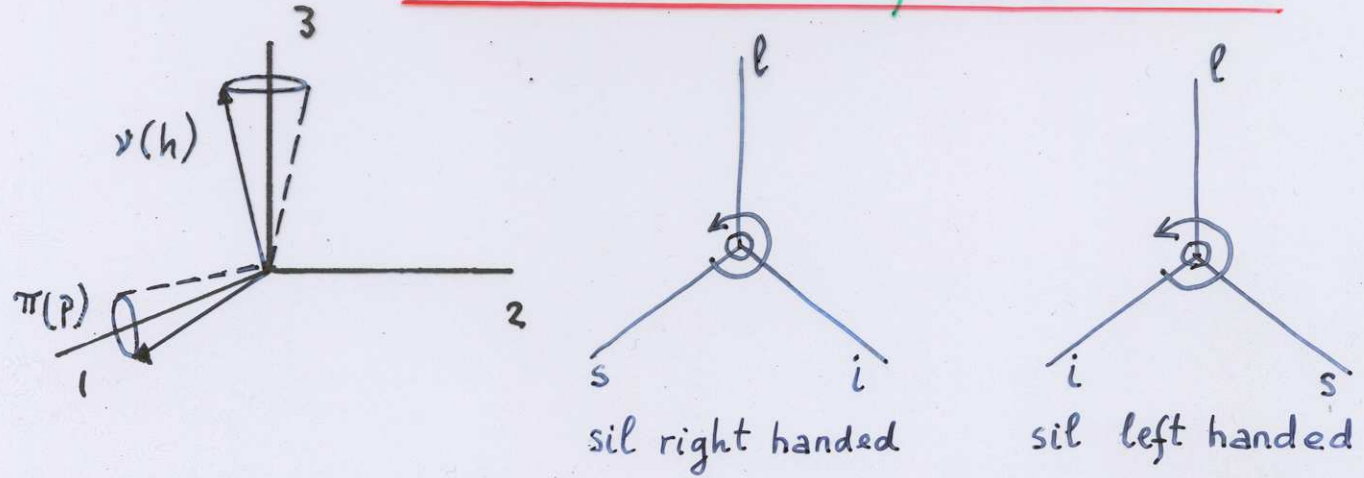


S.Frauendorf - EB meeting (1996) ; Nucl. Phys. A617 (1997) 131
 CORE $\rightarrow \frac{J_1}{J_3} = \frac{J_3}{J_2} \rightarrow$ 2-axis

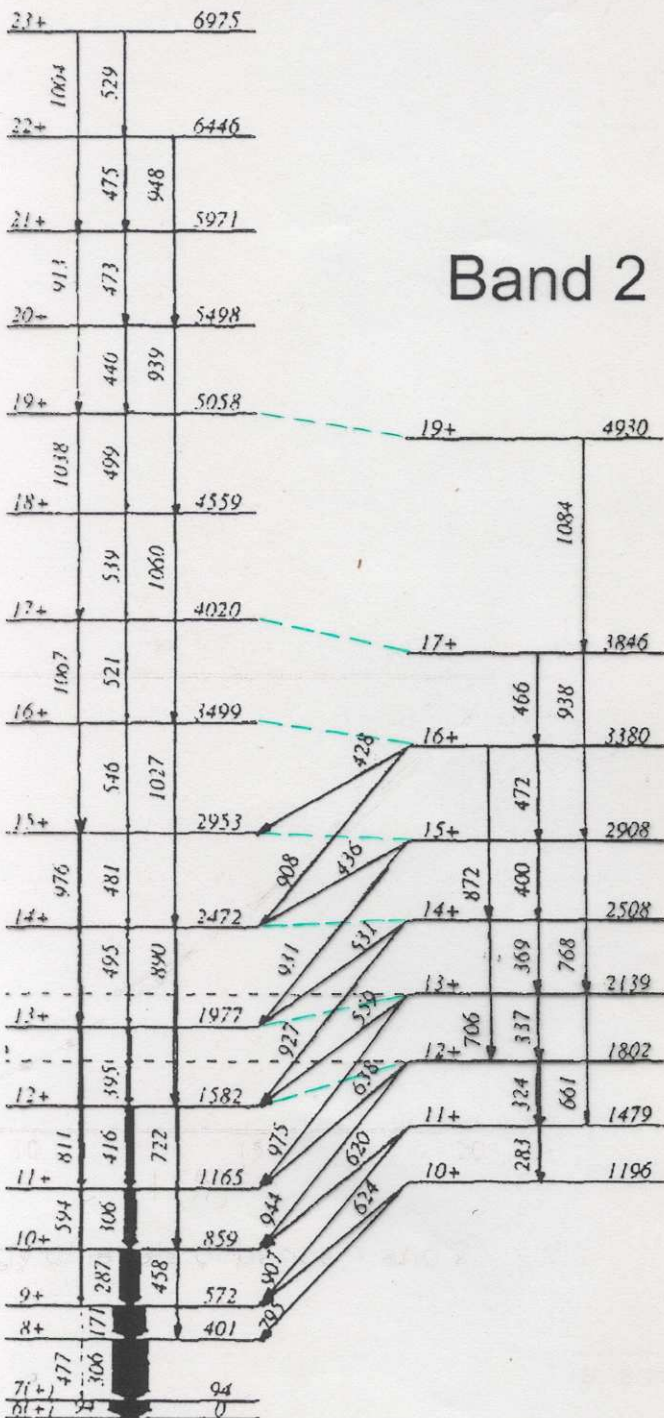


Chiral doublets of $\Delta I=1$ bands

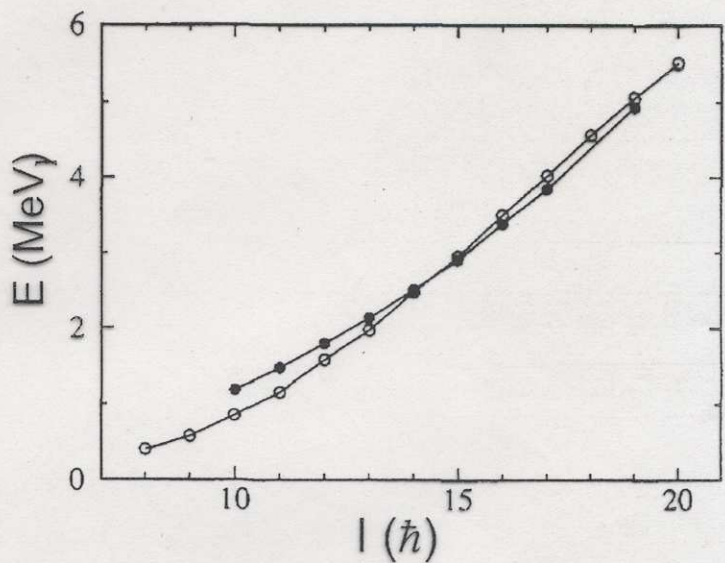


134 Pr

Band 1 $\tilde{\pi}h_{11/2} \otimes \tilde{v}h_{11/2}$



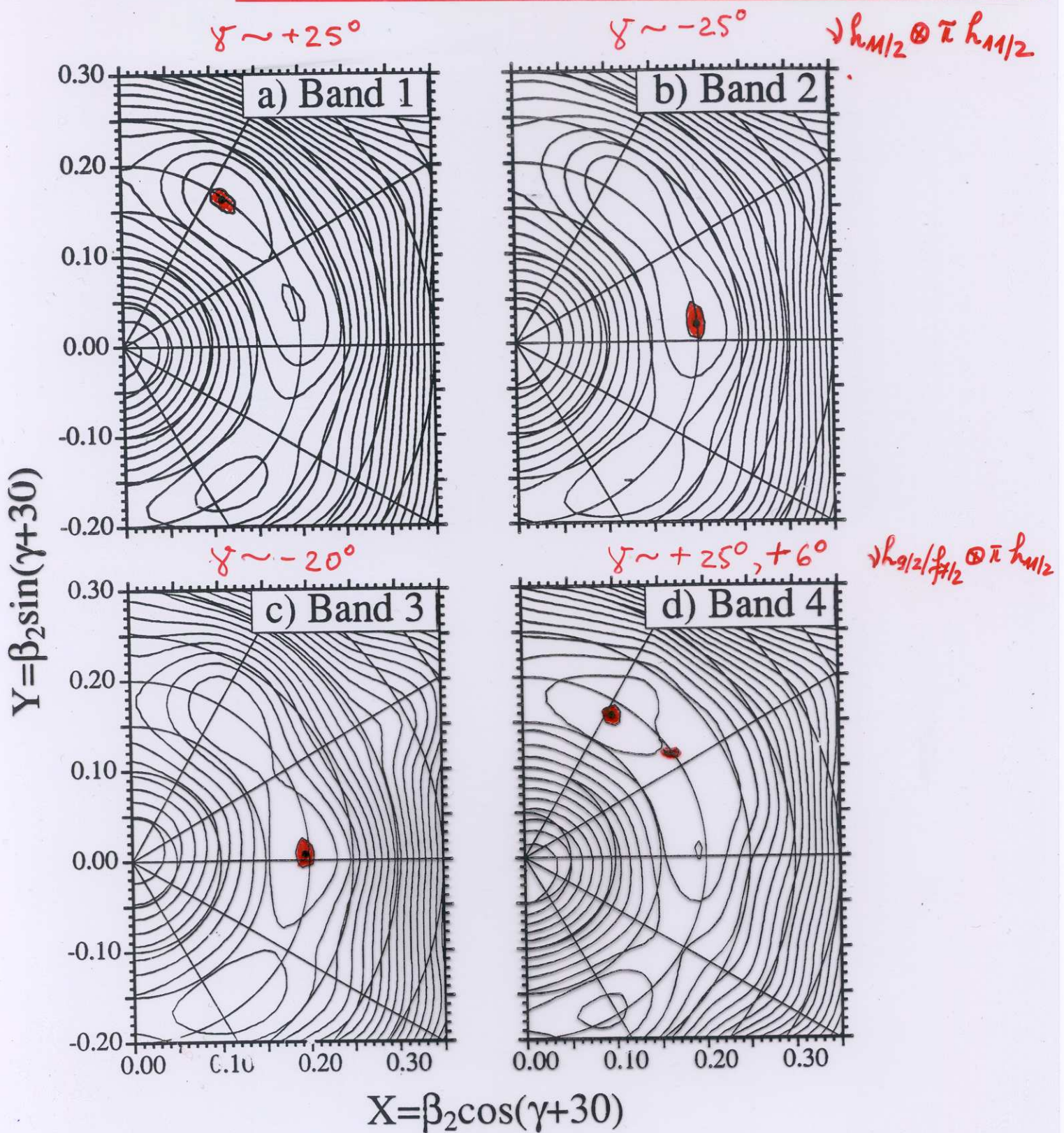
Band 2

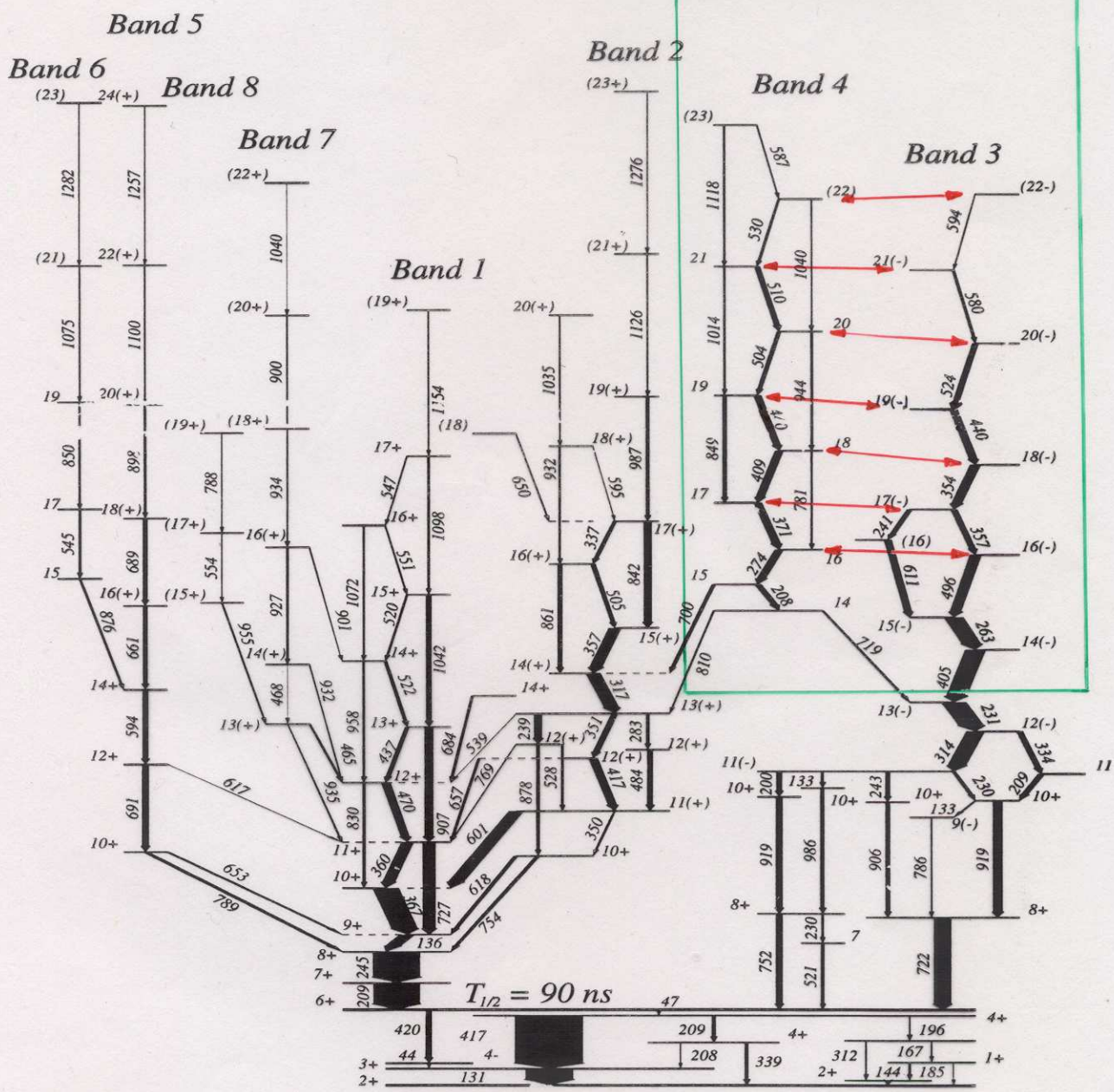


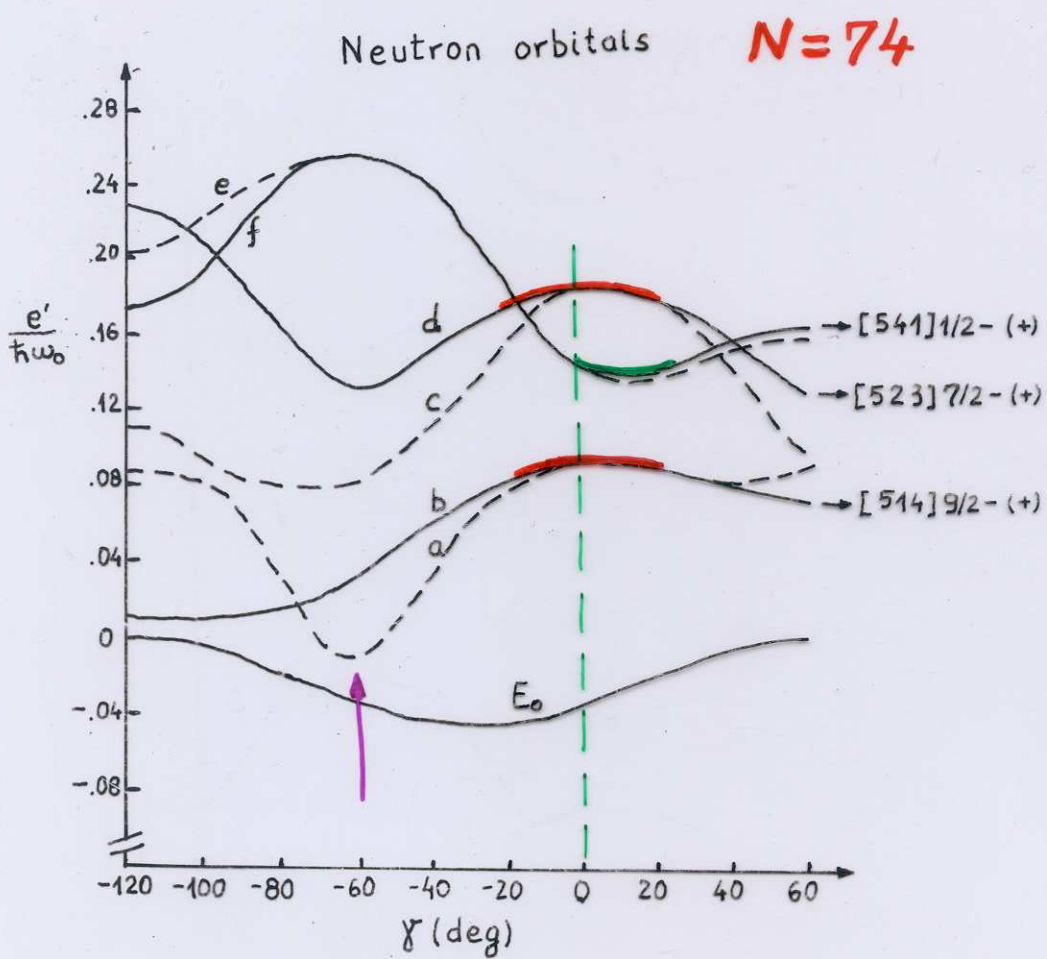
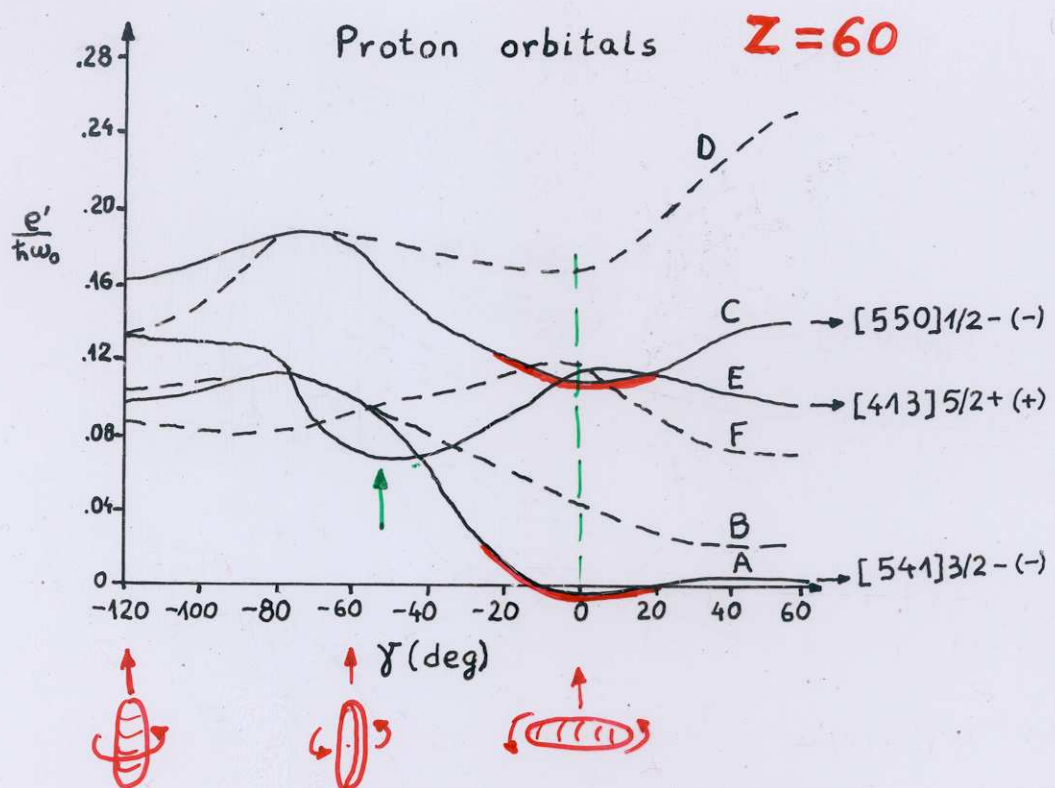
Energy of levels of bands 1 and 2.

Partial level scheme of ^{134}Pr
(C.M.Petrache et al. Nucl. Phys. A 597 (1996) 106)

Total routhian surfaces for ^{134}Pr



^{136}Pr Chiral doublet


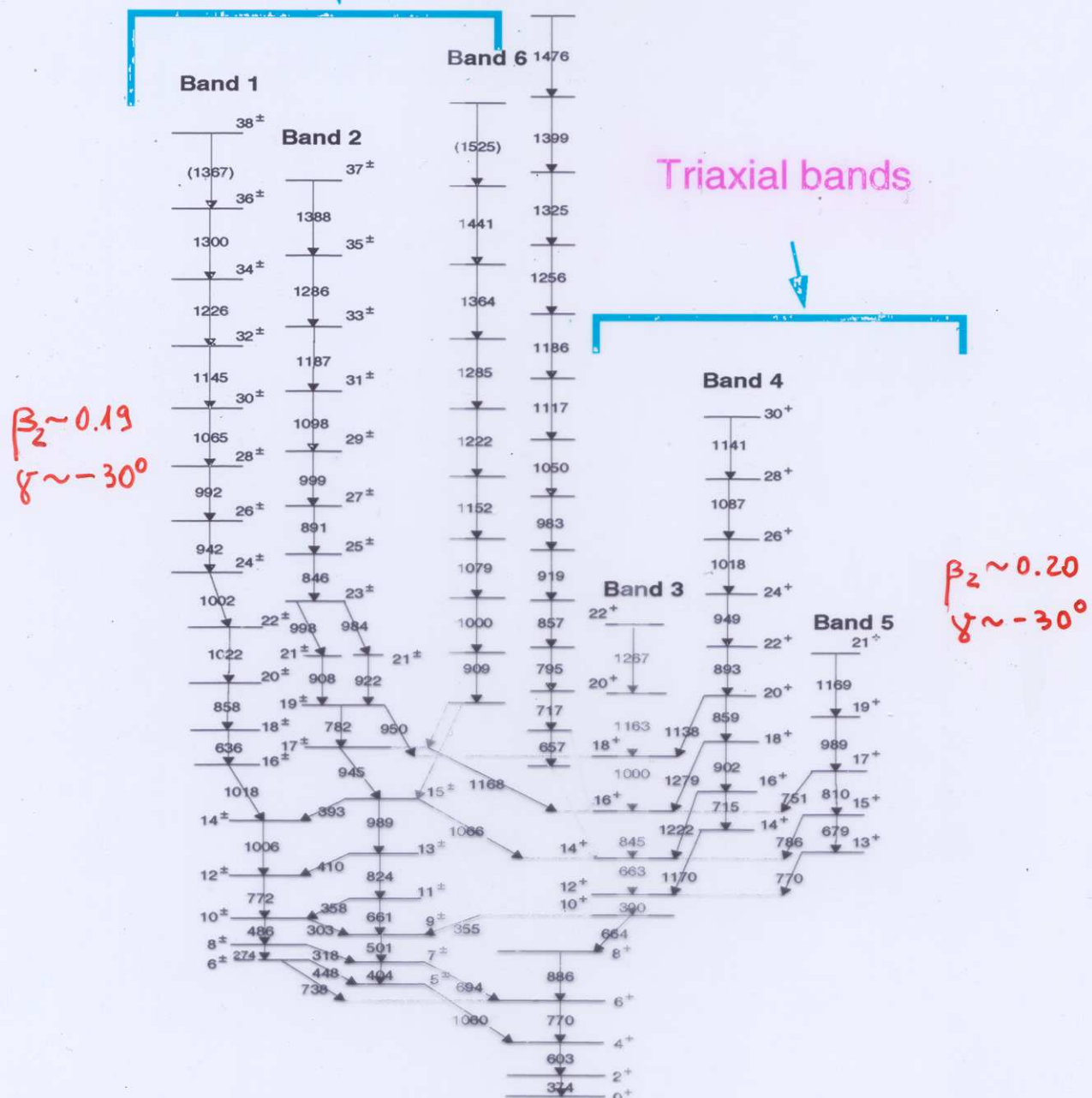


$$\varepsilon_2 = 0.2$$

^{136}Nd E2 bands

Triaxial bands $\beta_2 = 0.31$

Yrast SD band



C.M.P. et al.

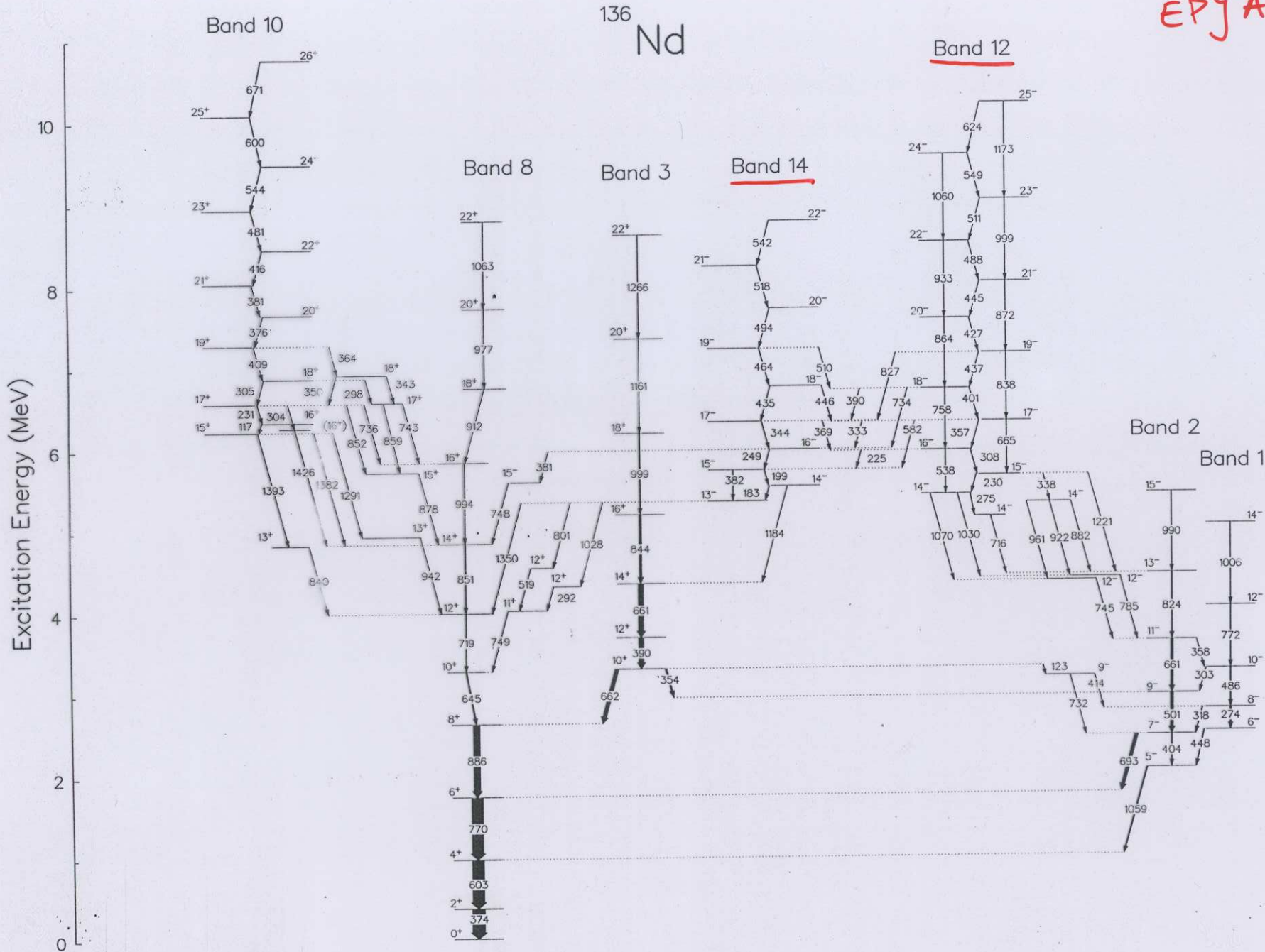
Phys. Lett. B 373 (1996) 275

E.S. Paul et al., Phys. Rev. C 36 (1987) 153

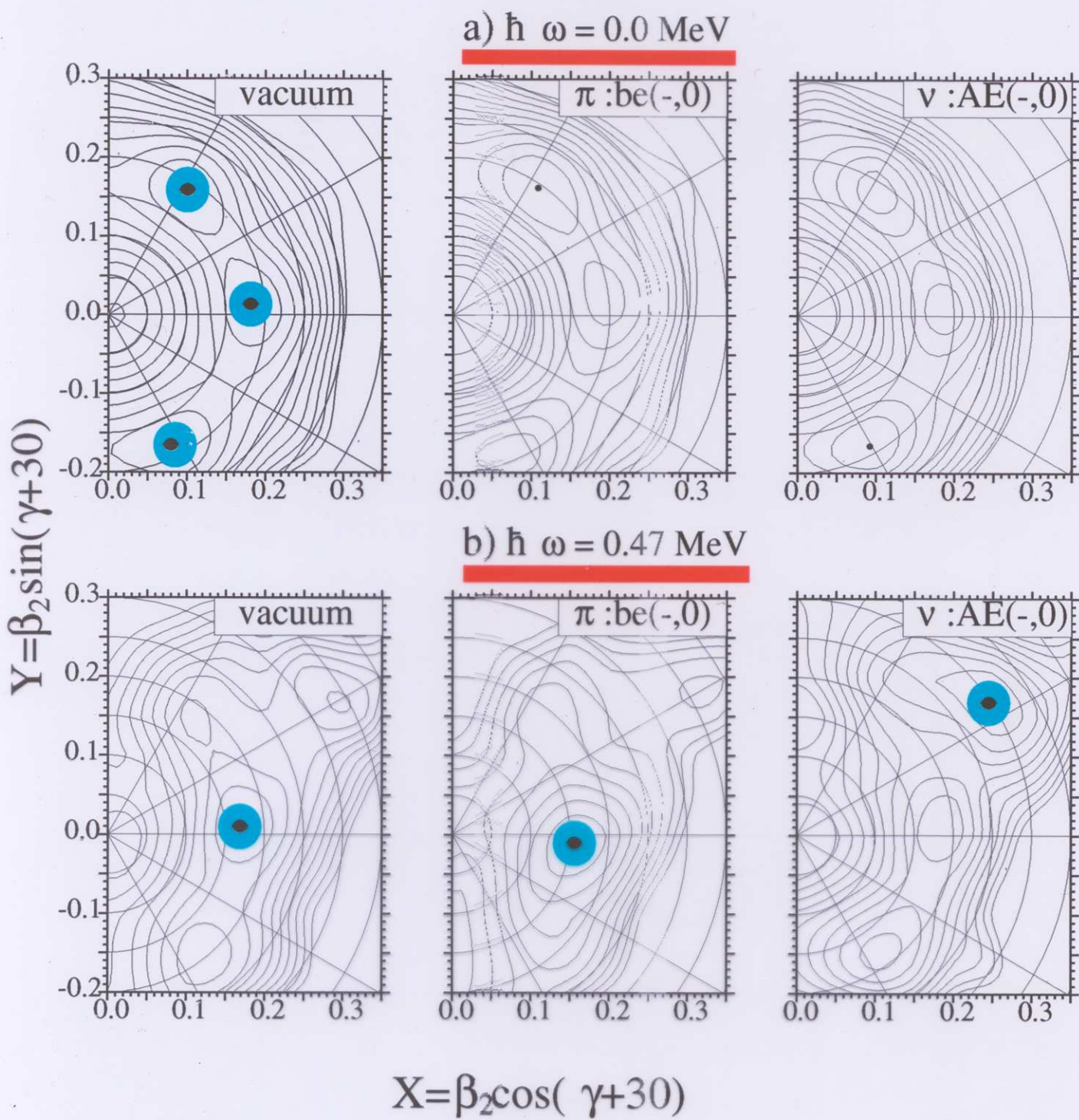
R.M. Clark et al., Phys. Lett. B 343 (1995) 59

C.M.P. et al., Phys. Rev. C 53 (1996) R2581

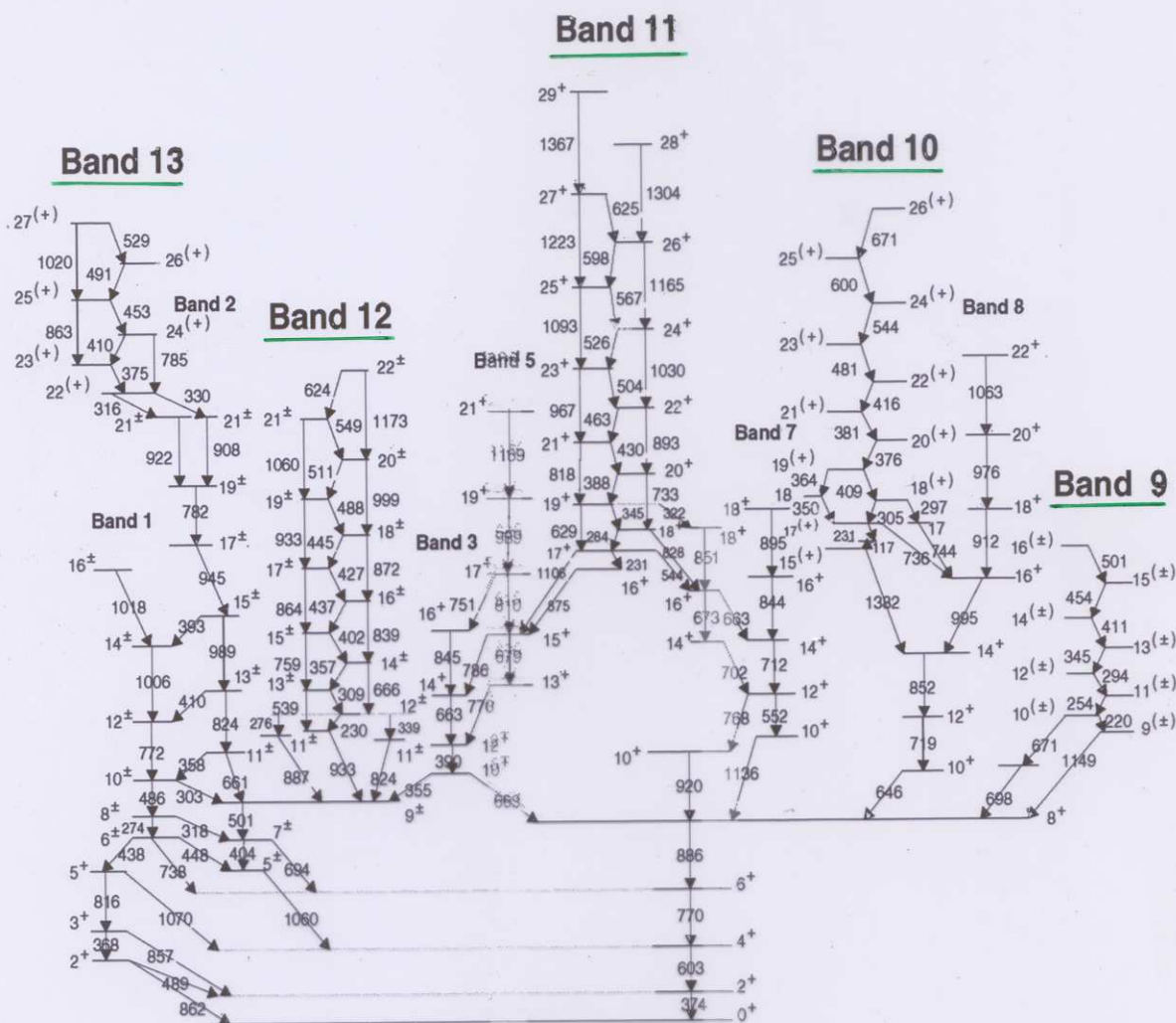
E. Mergel et al.,
EPJA last issue



Total routhian surfaces for different configurations in ^{136}Nd



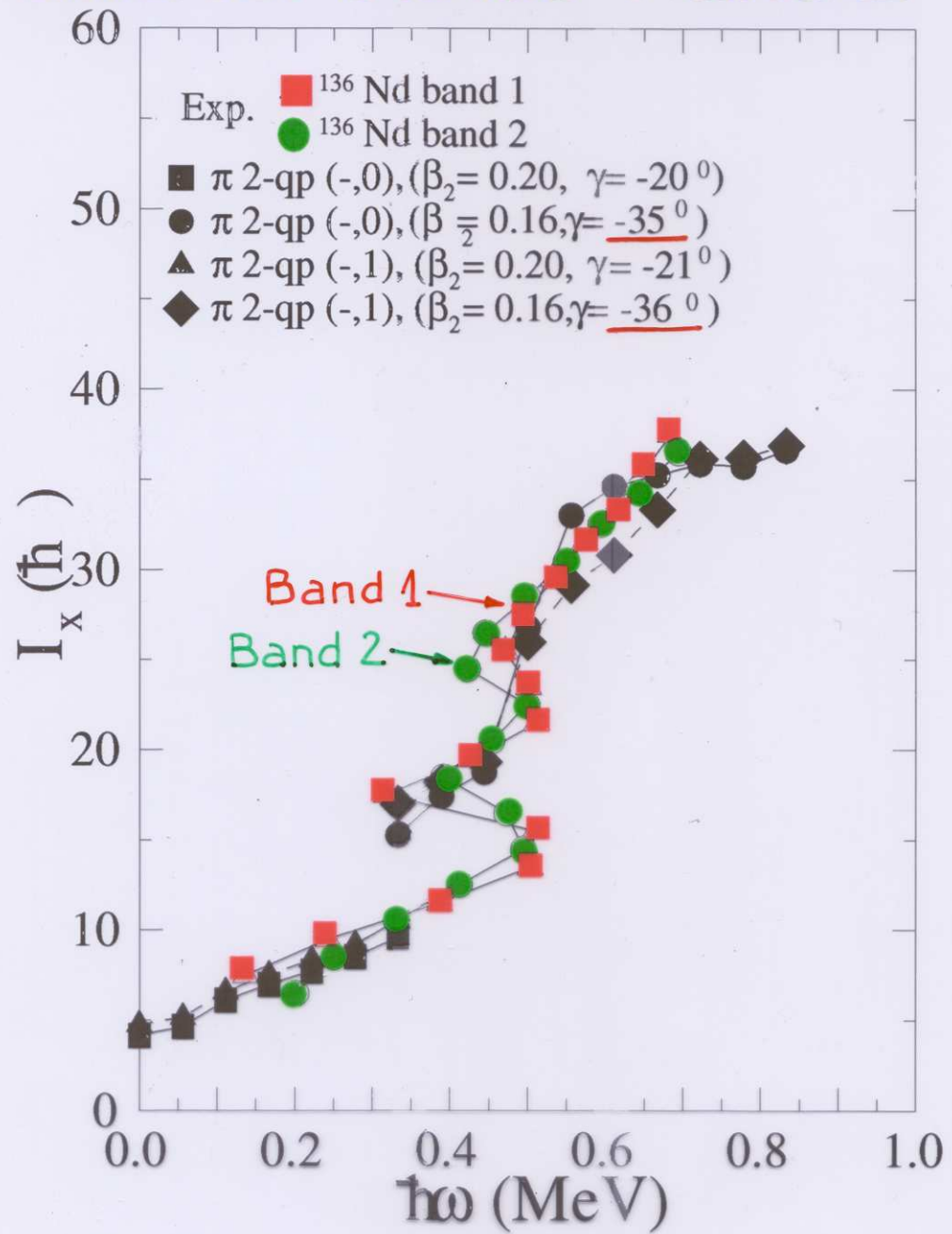
^{136}Nd M1 bands

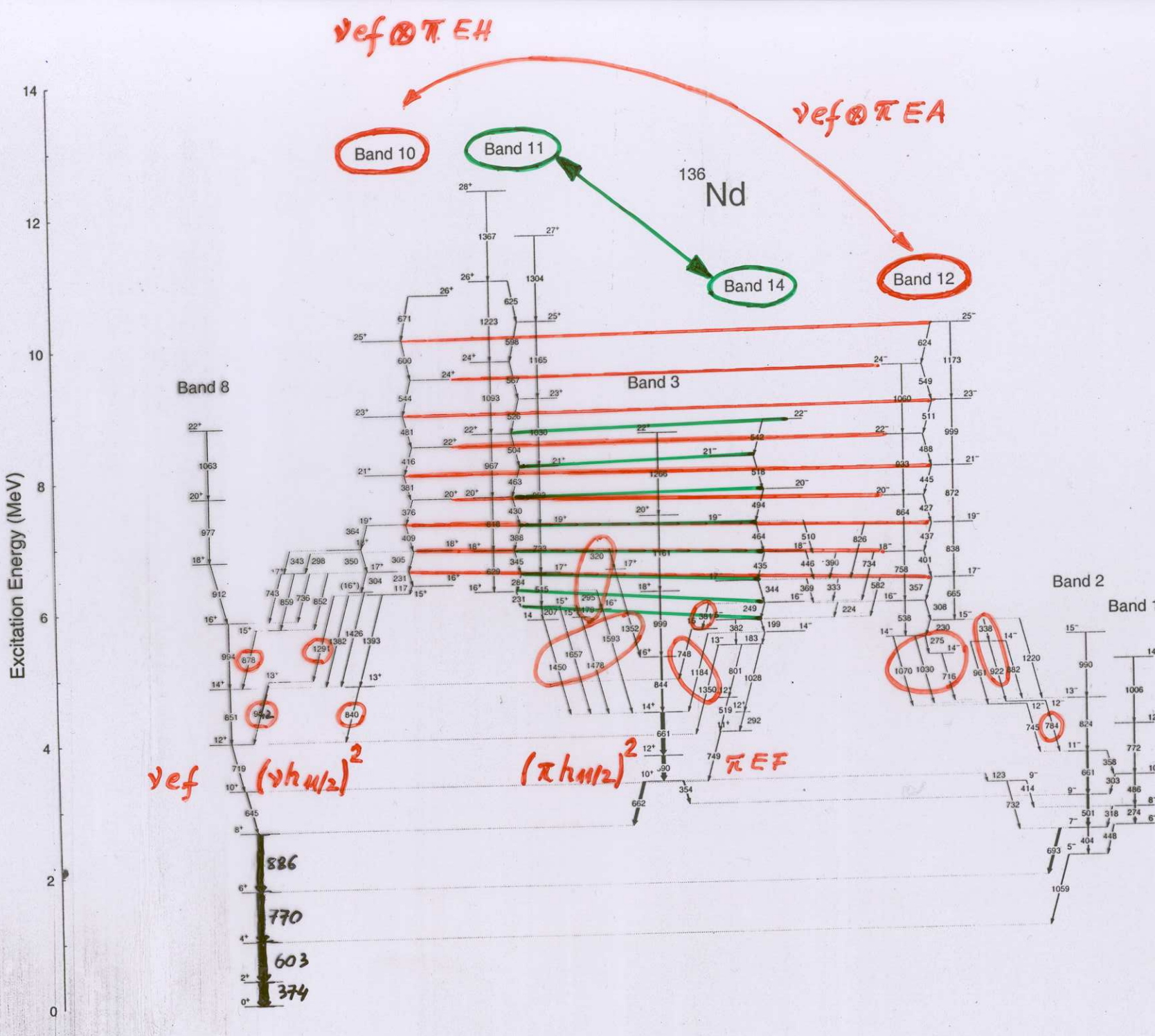


C.M.P. et al.

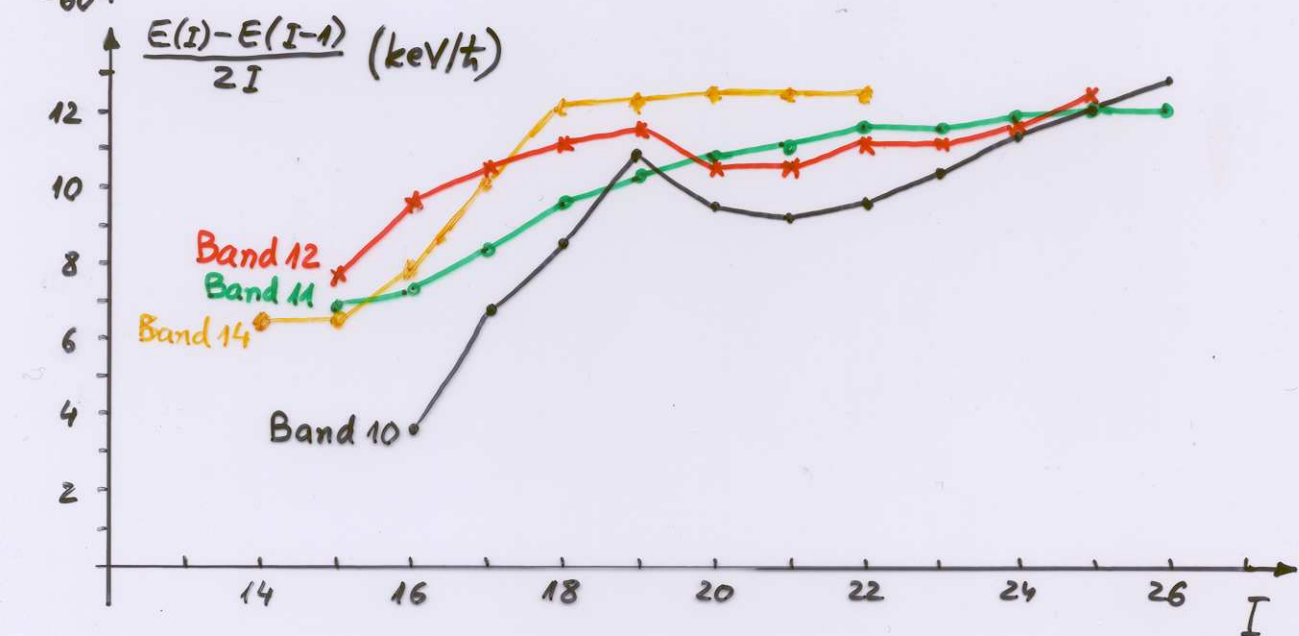
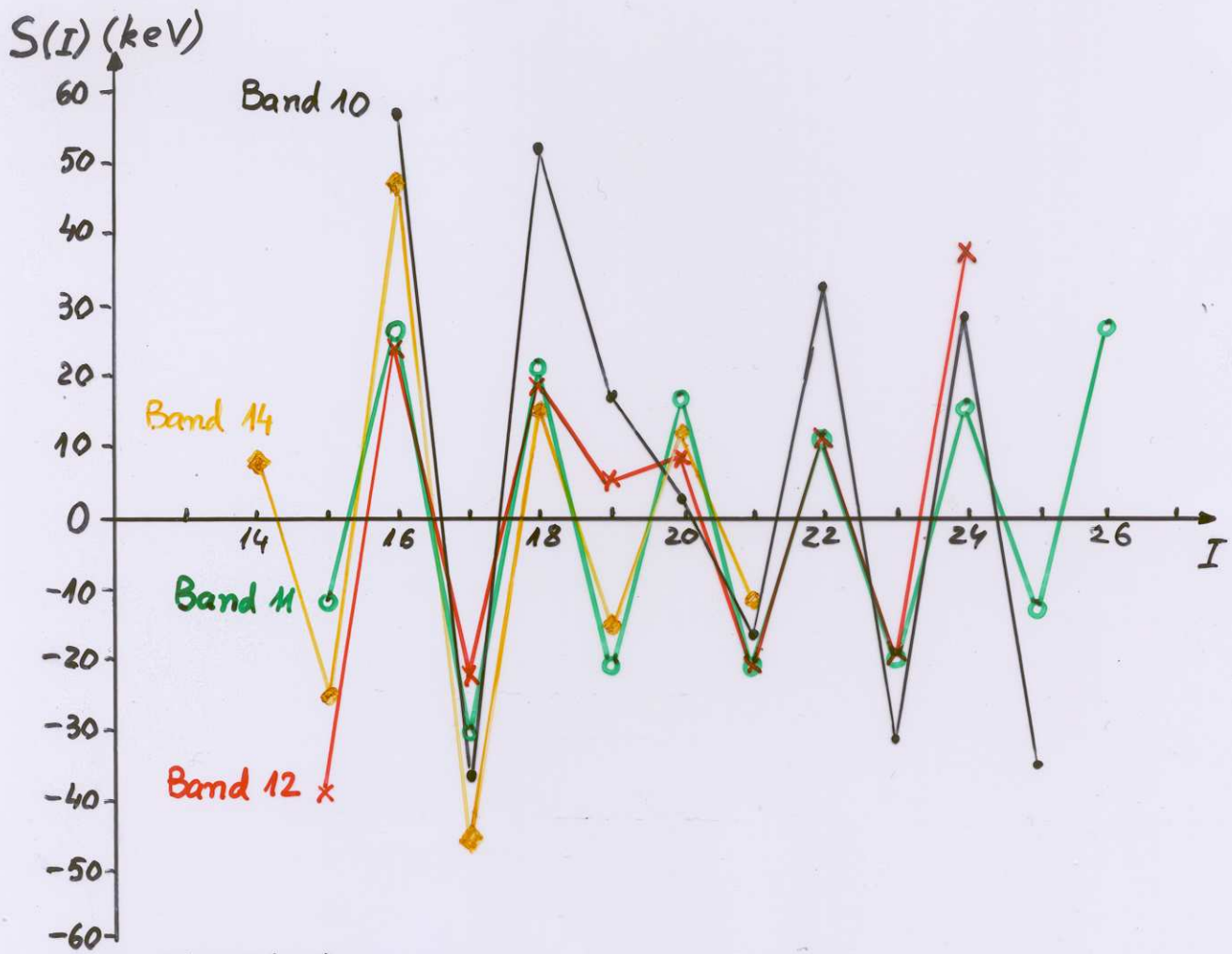
Phys. Rev. C53 (1996) R2581

Spin along the rotational axis for bands 1 and 2





$$S(I) = \frac{E(I+1) - E(I-1)}{2} - E(I)$$



Nuclear Tetrahedral Symmetry

J. Dudek, June 2002

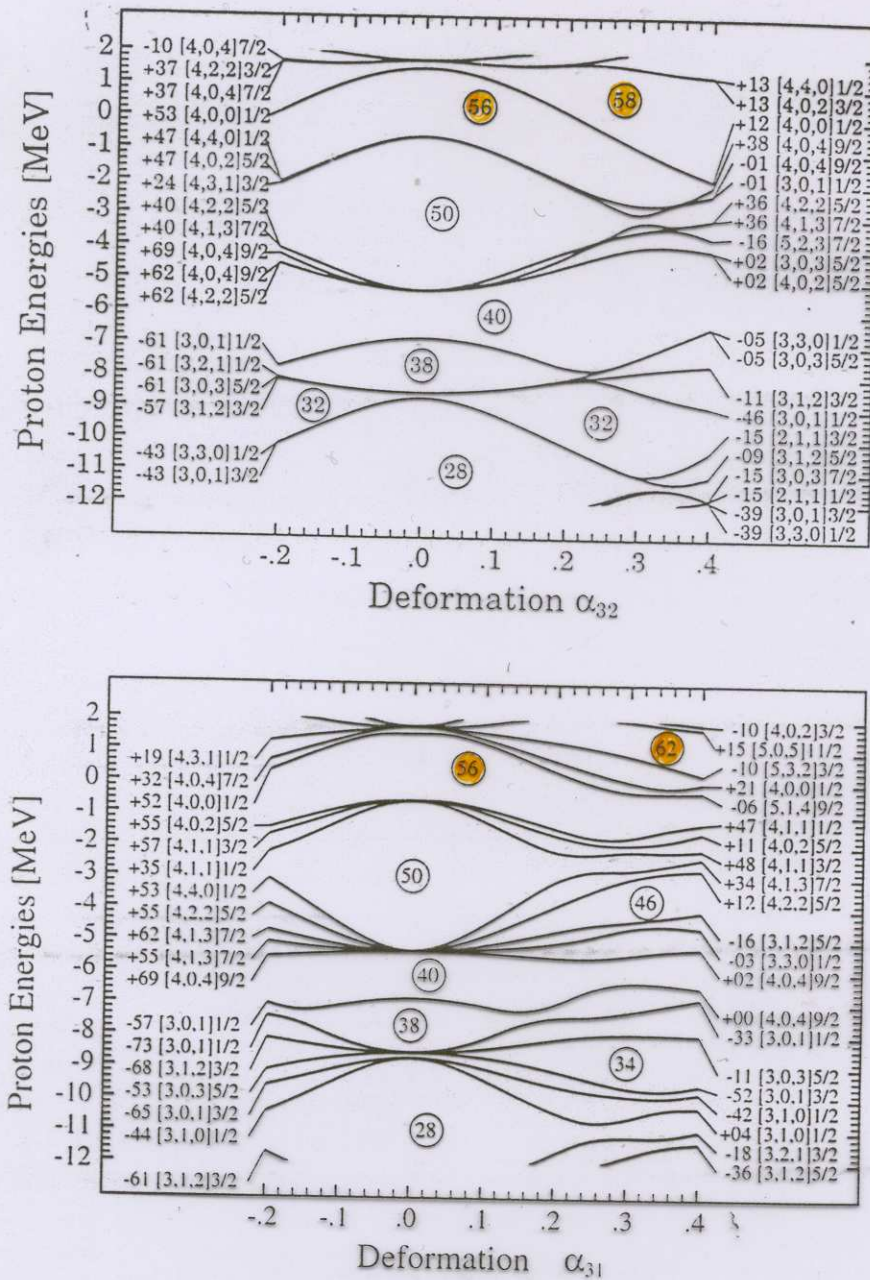


FIG. 1. Results of the realistic calculation of the proton single-particle energies in function of the α_{32} deformation corresponding to the T_d^D symmetry (top) compared to the analogous dependence in function of α_{31} (bottom, C_{2v}^D group). The numbers in front of the Nilsson labels give the expectation values of parity at the extremes of the deformation axes. None of the Nilsson quantum numbers is a good quantum number at tetrahedral deformations: Each label gives the full set of quantum numbers of the strongest basis state. (Results were obtained using a standard deformed Woods-Saxon potential.)

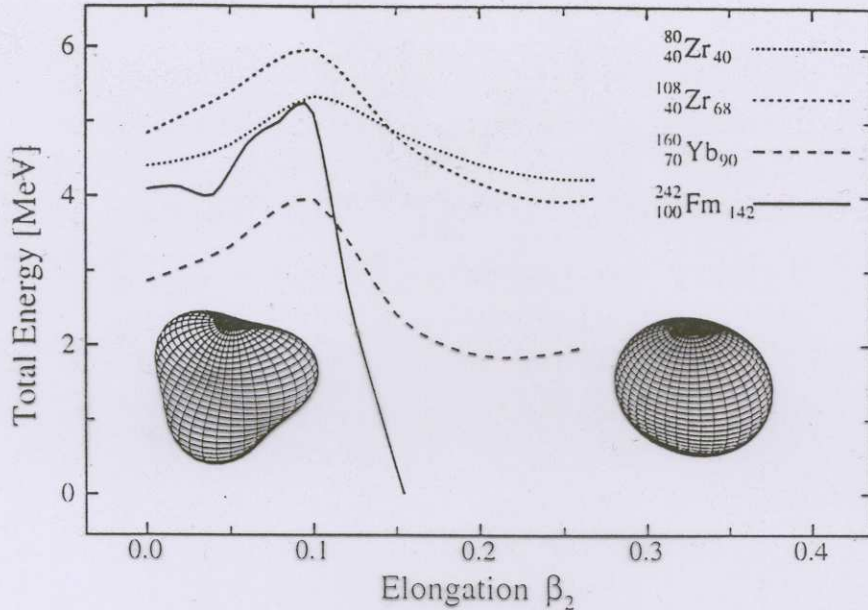


FIG. 2. Results of the multidimensional minimization of the total nuclear energies projected on the quadrupole deformation axis. The gamma deformation as well as all other deformations vary along the β_2 axis following the minimization, for each curve separately. The left-hand side inset shows an exaggerated (for better visibility) view of the tetrahedral shape at $\alpha_{32} = 0.3$, roughly twice the calculated equilibrium deformation. The right-hand side inset shows for comparison an oblate shape surface at $\beta_2 = 0.20, \gamma = 60^\circ$, i.e., roughly at the calculated equilibria.

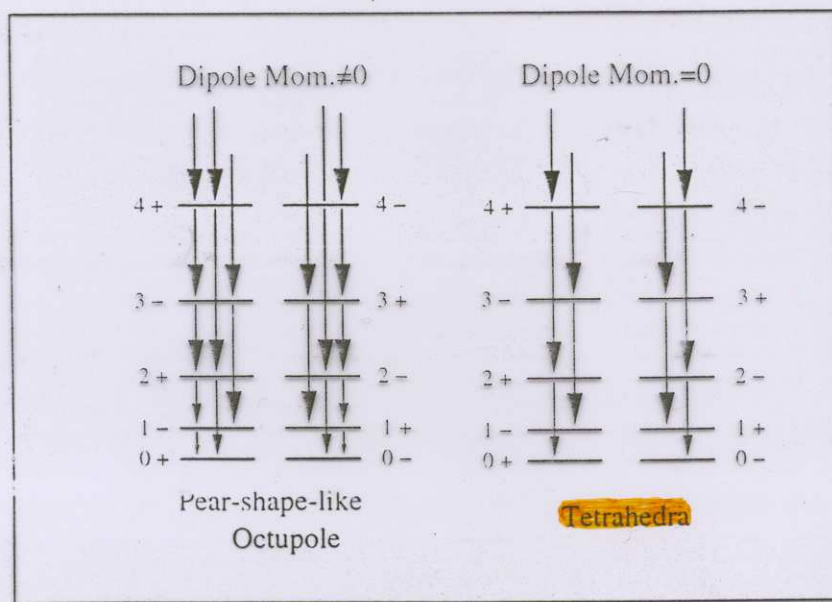
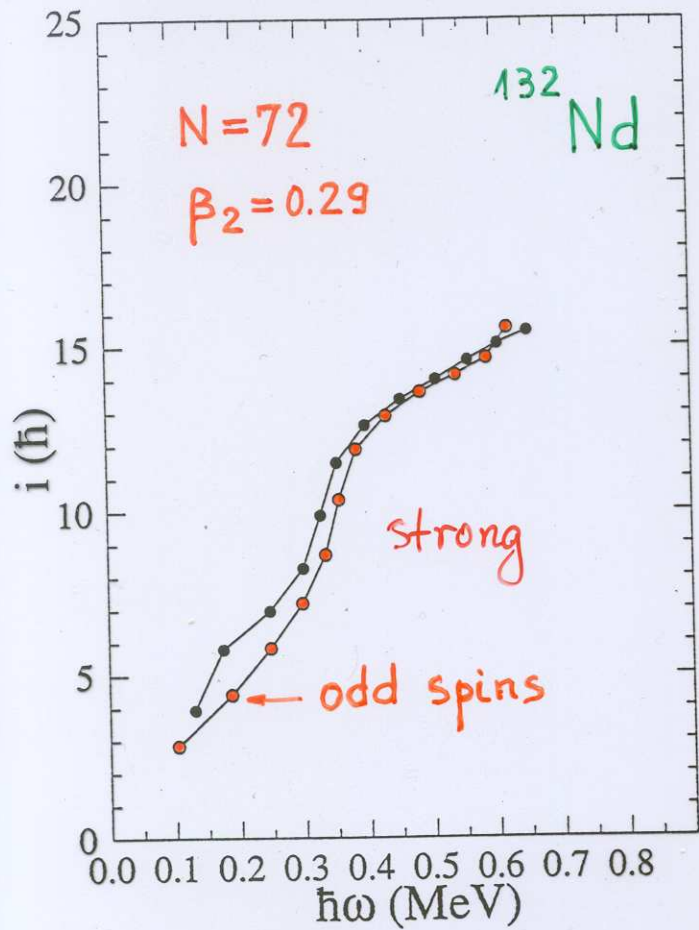


FIG. 3. Qualitative comparison of the electromagnetic transitions in a “pear-shape” nucleus, left, and a tetrahedral nucleus, right. In the former case, the static dipole moments are often strong, thus implying a presence of the collective interband $E1$ transitions in addition to the $E2$ ones. Tetrahedral nuclei generate no static dipole moments and, thus the $E1$ transitions should be absent in this case.

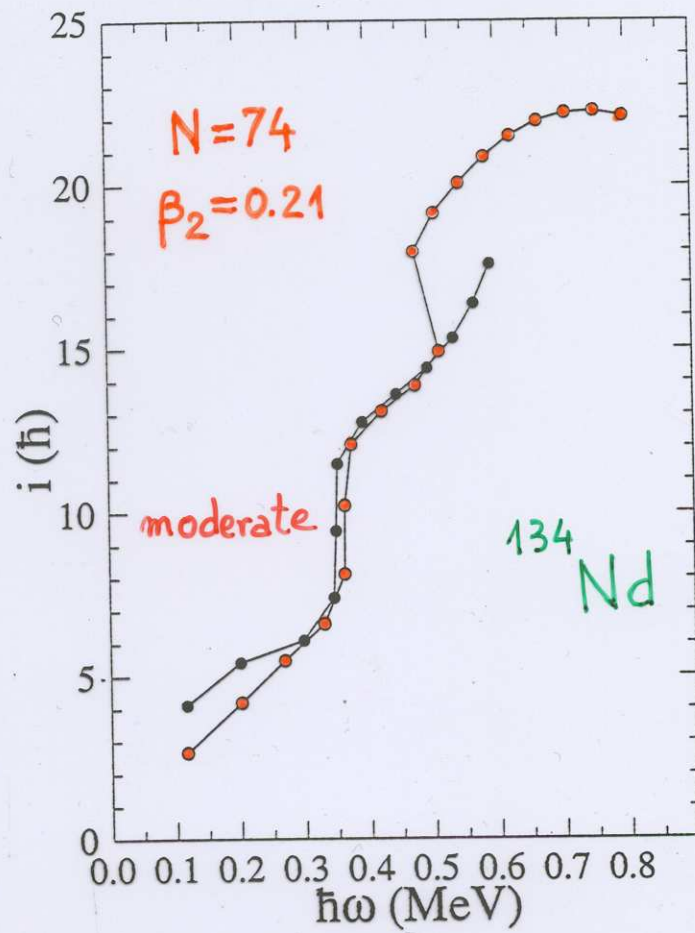
Experimental identification of T_d^D

1. Within the class of single-particle excit.,
the 4-fold degeneracies \Rightarrow
*multitude of particle-hole transitions
of close-lying energies*
*in some cases \Rightarrow 16-fold degenerate
multiplet of transitions*
2. Within the class of low-lying collective
rotational excitations \Rightarrow
*simplex symmetry \rightarrow parity-doublet bands
without E1 interband transitions*

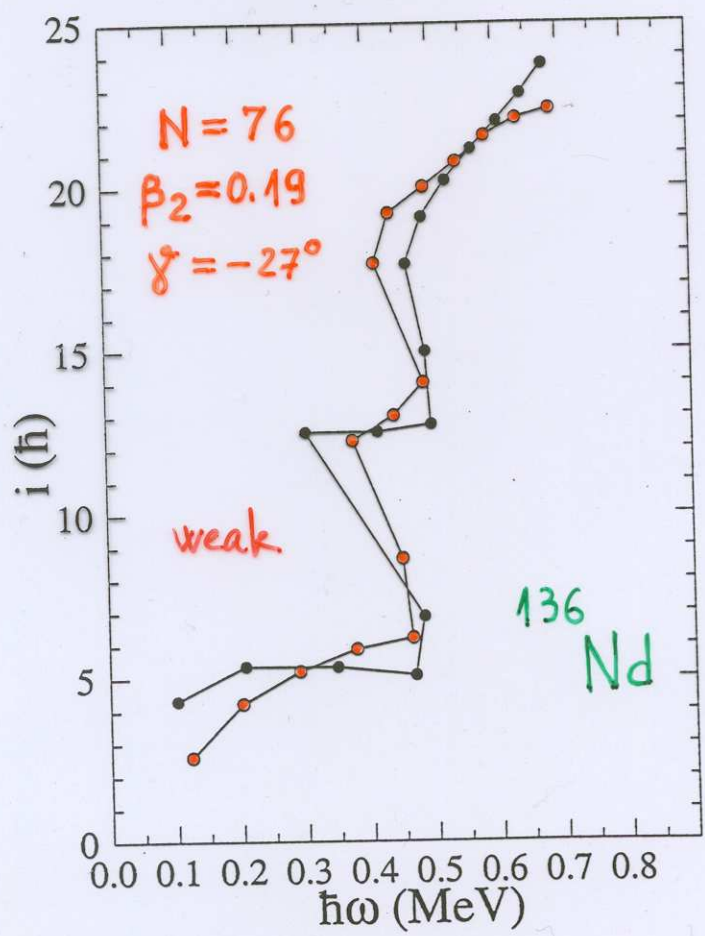
Alignments of the Bands 1 and 2 in ^{132}Nd



Alignments of the Bands 1 and 2 in ^{134}Nd



Alignments of the E2 Bands in ^{136}Nd

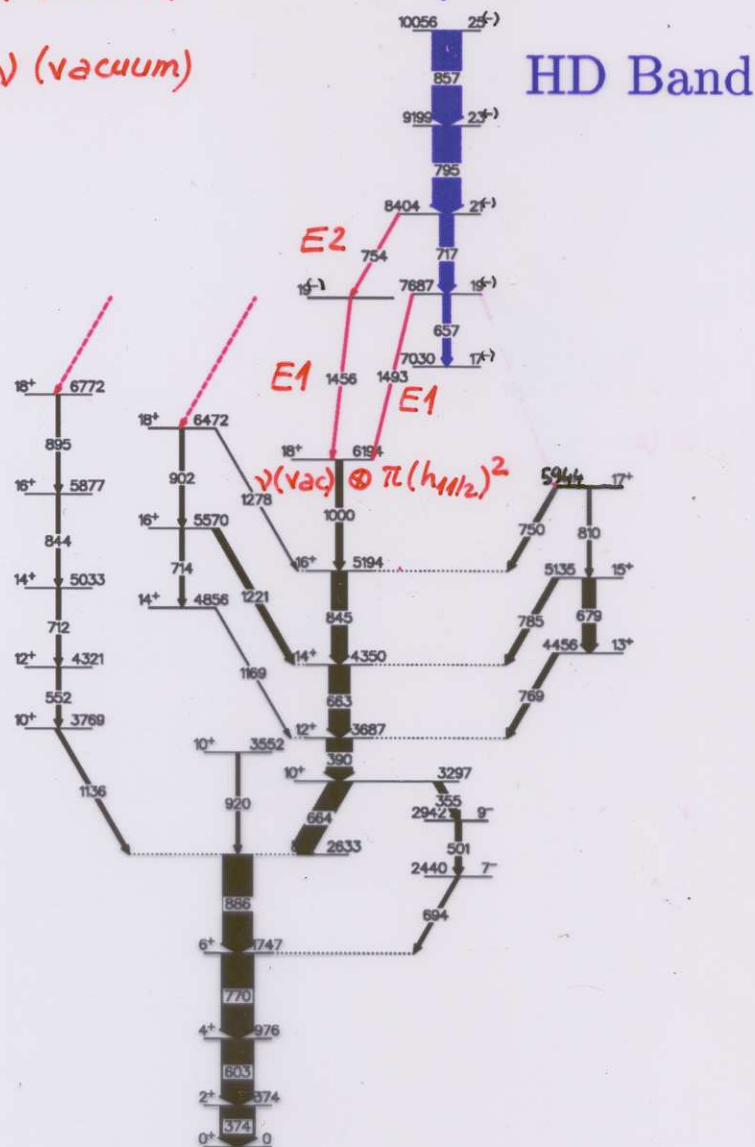


136Nd decay-out level scheme

$\downarrow i_{13/2} h_{9/2} \xrightarrow{\Delta j=2^-} \downarrow (\text{vacuum})$

$\downarrow i_{13/2} f_{7/2} \xrightarrow{\Delta j=3^-} \downarrow (\text{vacuum})$

$\downarrow i_{13/2} h_{9/2} / f_{7/2} \otimes \pi(h_{11/2})^2$



DCO measurements \Rightarrow 1456 keV $\Delta I=1$
754 keV $\Delta I=2$

→ The band disappears at spin 17^- with an excitation energy of 7030 keV

→ Decay-out pattern similar to ^{134}Nd

390-662.cmat Cut of 844.0 keV

